Measurement of Ice Growth During Simulated and Natural Icing Conditions Using Ultrasonic Pulse-Echo Techniques

R. John Hansman Jr.* and Mark S. Kirby†
Massachusetts Institute of Technology, Cambridge, Massachusetts

Results of tests to measure ice accretion using ultrasonic pulse-echo techniques are presented. Tests conducted on a 10.2-cm (4-in.) -diam cylinder exposed to simulated icing conditions in the NASA Lewis Icing Research Tunnel and on an 11.4-cm (4.5-in.) -diam cylinder exposed to natural icing conditions in flight are described. An accuracy of ±0.5 mm (±0.02-in.) is achieved for ice thickness measurements. Ice accretion rate is determined by differentiating ice thickness with respect to time. Icing rates measured during simulated and natural icing conditions are compared and related to icing cloud parameters. The ultrasonic signal characteristics are used to detect the presence of surface water on the accreting ice shape and, thus, to distinguish between dry ice growth and wet growth. The surface roughness of the accreted ice is shown to be related to the width of the echo signal received from the ice surface.

Nomenclature

C = speed of propagation of ultrasonic compressive wave
D = ice thickness
LWC = liquid water content of cloud
MVD = median volume diameter of cloud droplets
T = cloud temperature
$T_{p\text{-}e}$ = pulse-echo time
V = freestream airspeed

Introduction

THE purpose of the tests described herein was to investigate the application of the ultrasonic pulse-echo technique to the measurement of dynamically changing ice thickness. Since this technique provides a continuous measurement of ice thickness, it possesses a unique capability to accurately resolve ice growth. This information would be extremely valuable to support and validate both analytical and experimental ice modeling efforts. Ultrasonic pulse-echo ice thickness measurement could also provide the basis for the development of an operational instrument to detect and accurately measure ice thickness and accretion rate on critical aircraft components.

Ultrasonic pulse-echo measurement of ice thickness on a surface is accomplished by emitting a brief compressive wave or pulse from an ultrasonic transducer mounted flush with the accreting surface (Fig. 1). The pulse travels through the ice, is reflected at the ice/air interface, and then returns to the transducer as an echo signal. The time elapsed, $T_{p\text{-}e}$, between the emission of the pulse from the transducer and the return of the echo from the ice interface can then be used to calculate the ice thickness D using the following formula:

$$D = CT_{p\text{-}e}/2 \tag{1}$$

where C is the speed of propagation of the pulse-echo signal in ice. It has previously been shown[1-4] that the speed of propagation is insensitive to the different types of ice (glaze, rime, and mixed) formed at typical flight velocities; a value of 3.8 mm/μs is used for all of the results presented herein. Figure 1 also shows a typical pulse-echo signal obtained from a stationary, i.e., nonaccreting, ice surface.

Received Sept. 19,1985; presented as Paper 86-0410 at the AIAA 24th Aerospace Sciences Meeting, Reno, NV, Jan. 6-9,1986; revision received Feb. 11, 1986.

*Assistant Professor, Aeronautics and Astronautics. Member AIAA.
†Research Assistant, Aeronautics and Astronautics.

Ultrasonic Signal Characteristics for Dry and Wet Ice Growth

A discussion of the unique ultrasonic pulse-echo signal characteristics observed under different icing conditions is now presented. These signal characteristics enable the type of ice growth to be easily discerned and provide valuable real-time information about the condition of the ice surface.

Dry Ice Growth

When all of the droplets impinging at a given location on a body freeze on impact, the freezing fraction is unity and the ice surface formed is "dry." This form of ice accretion is referred to as "dry ice growth," and is characteristic of rime ice formation at low temperatures.

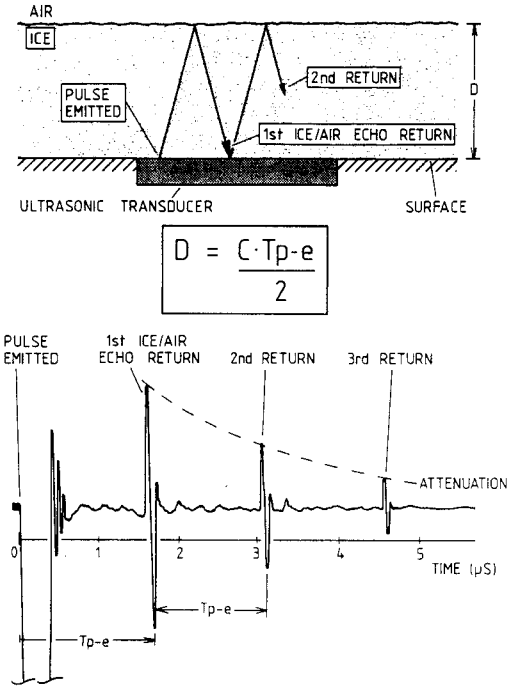

Fig. 1 Ultrasonic pulse-echo thickness measurement and typical ultrasonic pulse-echo signal in ice.

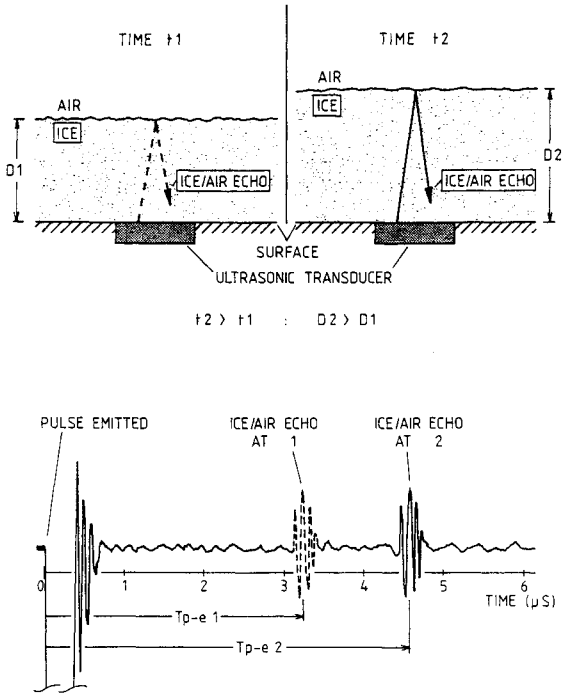

Fig. 2 Ultrasonic signal characteristics for dry ice growth.

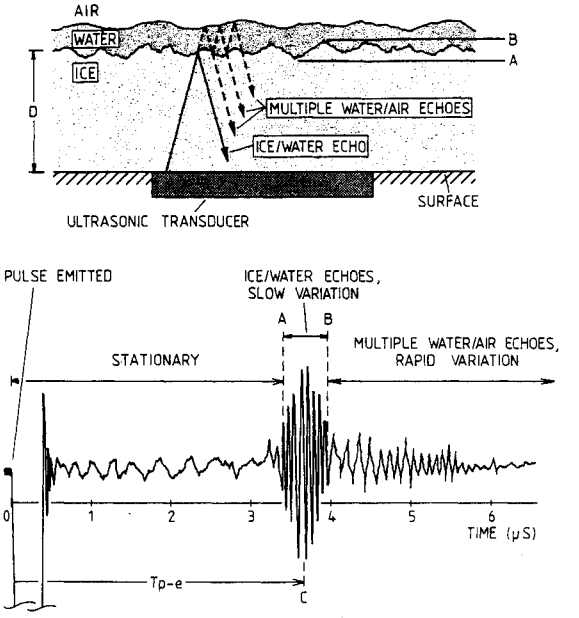

Fig. 3 Ultrasonic signal characteristics for wet ice growth.

The time taken for the impinging droplets to freeze under these conditions is so brief that the ice thickness measured simply appears to increase with time. Thus during dry ice growth the received echo signal simply appears to translate in time with a velocity proportional to the accretion rate. This behavior is illustrated in Fig. 2. Since the ice surface formed by dry ice growth is typically smooth, a sharp, well-defined echo is received, as shown in the figure.

Wet Ice Growth

When the heat transfer from the accreting surface is insufficient to completely freeze all of the impinging droplets, the freezing fraction is less than unity and liquid water will be present on the ice surface. This form of ice accretion is referred to as "wet ice growth," and is characteristic of glaze and mixed ice formation at temperatures just below 32°F. It should be noted that since the type of ice growth occurring, wet or dry, depends on the local collection efficiency and local heat-transfer coefficient, both of which may vary considerably over the body, it is quite possible to have wet growth at one location and dry growth at another. When this happens, the wet growth region is typically around the stagnation line of the body with dry growth occurring further "downstream" on the body. This behavior results in a relatively clear (glaze) ice formation in the wet growth region around the stagnation line and an opaque, milky (rime) ice structure further downstream where the ice growth is dry.

During wet ice growth the ice surface is covered, at least partially, by a thin liquid layer. The emitted ultrasonic pulse thus encounters two separate interfaces: an ice/water interface and a water/air interface, as shown in Fig. 3. Two echo signals are therefore received by the transducer; the first from the ice/water interface and a second, later echo from the water/air interface. The echo received from the ice/water interface is characteristically broader than the echoes received during rime ice growth due to the rougher ice surface formed during glaze icing. As in the rime ice case, this ice/water interface echo translates in time as liquid freezes at the interface and increases the accreted ice thickness. However, since different areas of the ice surface over the transducer freeze independently, the detailed shape of the ice/water echo slowly changes as the ice surface over the transducer constantly changes shape.

Since the liquid layer over the ice surface is thin, and its attenuation is low, many multiple echoes are received from the water/air interface following the ice/water echo. Due to distortion of the liquid surface by impinging droplets and the external flow, the shape of these multiple water/air echoes also changes as the instantaneous local thickness and surface orientation of the liquid layer vary. While the shape of the ice/water echo varies slowly, the shape of the water/air echoes varies rapidly, making it possible to clearly discern the transition between the ice/water echo "band" and the water/air echoes. The pulse-echo transit time to the ice/water interface can thus also be determined from the location of this transition point. The different rates at which the respective echoes change shape are due to the different physical processes involved at the two interfaces. The slow variation of the ice/water echo corresponds to a characteristic freezing time at that interface, while the rapid variation of the water/air echoes represents the distortion of the water/air surface, thought to be caused by the flowfield and impacting droplets.

As noted earlier, during dry ice growth the ice surface is relatively smooth and the pulse-echo time is correspondingly well defined. However, during wet growth the roughness of the ice surface increases the width of the echo signal and a consistent region of the ice surface echo must be selected to measure ice thickness (see Fig. 3). If the first echo return, labeled "A" in the figure, is selected, then the minimum thickness over the transducer will be recorded. Likewise the last ice surface echo return, "B," corresponds to the maximum ice thickness over the transducer. For all of the tests described herein, the central region of the ice surface echo, "C," was selected and, thus, the ice thickness measured represents an "average" ice thickness over the transducer area.

Experimental Apparatus

The experimental apparatus for both the Icing Research Tunnel (IRT) tests and the natural icing flight tests consisted of the following equipment:

1) A cylinder containing small ultrasonic transducers mounted flush with the cylinder surface.
2) A pulser/receiver unit to drive the transducers.
3) An oscilloscope to display the resulting pulse-echo signal.
4) A video-camera/recorder to record the pulse-echo signal

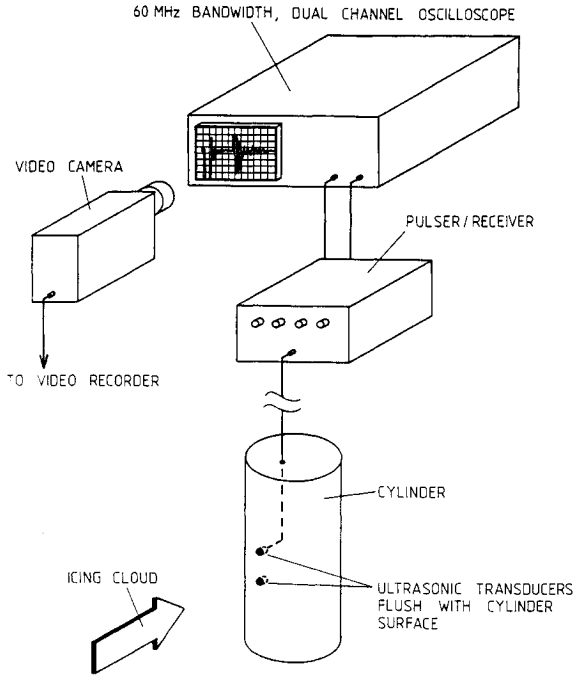

Fig. 4 Experimental apparatus configuration.

displayed on the oscilloscope.

Figure 4 schematically illustrates the configuration of the experimental apparatus used for both series of tests.

For the IRT tests a 10.2-cm (4-in.) -diam cylinder approximately 30.5 cm (12 in.) long was instrumented with four ultrasonic transducers. All of the transducers used had plane circular faces with element diameters of either 0.6 or 1.3 cm (0.25 or 0.5 in.). The transducers had center frequencies of 1, 2.25, and 5 MHz; all were broadband, heavily damped transducers. As expected, the 5-MHz transducers provided the highest thickness resolution (due to the smaller wavelength); all results presented are for 5 MHz transducers. The transducers were placed on the stagnation line of the cylinder, and all were located near the midsection of the cylinder to minimize distortion of the ice accretion due to three-dimensional tip effects. A pulser/receiver unit provided the electrical signals necessary to generate the ultrasonic pulse and amplify the return echo.

The cylinder employed for the natural icing flight tests was an 11.4-cm (4.5-in.) -diam cylinder, 38.1 cm (15 in.) long. This cylinder was instrumented with two 0.6-cm (0.25-in.) -diam, 5-MHz transducers. Both transducers were mounted on the stagnation line of the cylinder, equispaced 5.1 cm (2 in.) about the cylinder midsection. A single pulser/receiver unit was used to drive either transducer.

In order to observe the ultrasonic signal characteristics in detail, an oscilloscope was used in both series of tests to display the pulse-echo signal. A video camera was focused on the oscilloscope screen and used to record this signal permanently. The video camera simultaneously recorded the cylinder exposure time from an electronic clock.

Testing

Icing Research Tunnel Tests

The 10.2-cm (4-in.) cylinder instrumented with ultrasonic transducers was vertically suspended from the roof of the IRT, as shown schematically in Fig. 5. In order to allow another experiment unobstructed access to the icing cloud, the cylinder did not extend into the calibrated region of the cloud. The cylinder was exposed to the icing cloud, and the pulse-echo signals from the two transducers being compared were recorded using the video camera/recorder. Each exposure, or run, was made with constant icing cloud parameters and typically lasted 8 min. At the completion of a run (or series of runs) the iced diameter of the cylinder at each transducer location was measured using a pair of outside calipers. The ice thickness over the transducers was inferred from this measurement for comparison with the ultrasonically measured ice thickness. The cylinder was then completely deiced in preparation for the next run. Ice growth for a total of 15 different icing cloud parameter sets, ranging from glaze to rime icing conditions, was recorded using the utrasonic pulse-echo system.

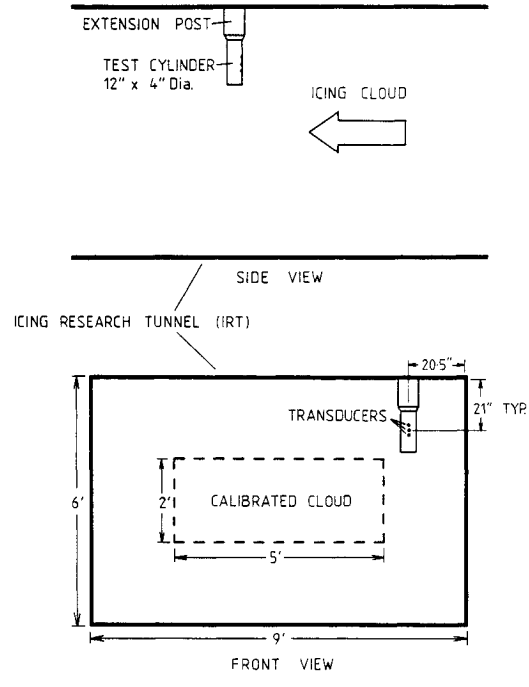

Fig. 5 Test cylinder installation for icing tunnel (IRT) tests.

Natural Icing Tests

Natural icing tests were conducted in flight from the NASA Lewis Icing Research Aircraft, a De Havilland Twin Otter. The 11.4-cm (4.5-in.) cylinder instrumented with ultrasonic transducers was exposed to icing conditions at the end of an extension post that was vertically extended through the roof of the aircraft by an experiment carrier mounted in the aircraft (see Fig. 6). The cylinder midsection was located 53.3 cm (21

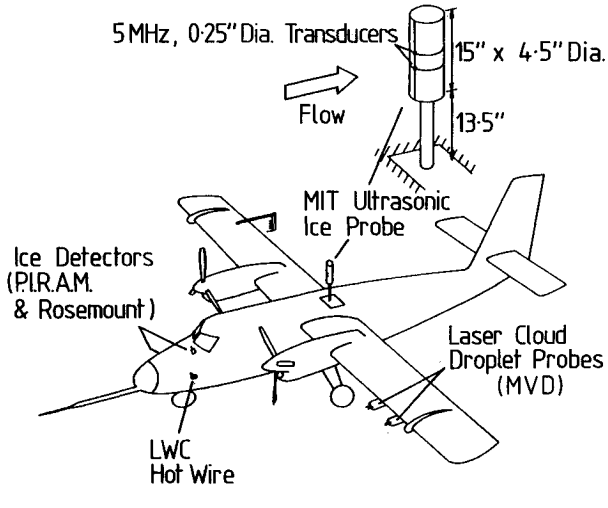

Fig. 6 Test cylinder installation for natural icing (NASA Lewis Twin Otter aircraft) tests.

in.) into the freestream when extended. A limit switch on the experiment carrier was used to synchronize the exposure time of the cylinder with icing cloud data acquired from other instruments during flight. The cylinder was typically exposed throughout the entire icing encounter, the pulse-echo signal again being continuously displayed and recorded by the oscilloscope/camera system. At the end of the encounter, the cylinder was retracted into the aircraft and the ice thickness over the transducer was measured using outside calipers. A total of four research flights were conducted with the ultrasonic system during the period March 30-April 2, 1985.

Results and Discussion

Icing Research Tunnel Tests

Figures 7 and 8 show ice thickness measured with the ultrasonic system plotted against exposure time for two different icing cloud parameter sets, labeled "heavy" and "light" icing, respectively. The heavy icing conditions represent an icing cloud with a high liquid water content (LWC) and a large median volume diameter (MVD) droplet size; whereas the light icing conditions represent relatively lower values for both of these parameters. The freestream airspeed was 230 mph for all of the heavy and light icing cases shown. Since the test cylinder was located outside the calibrated cloud (see Fig. 5), the values listed in Figs. 7 and 8 for icing cloud conditions are only approximate. In particular, the liquid water content was estimated to be approximately 50% of that in the calibrated region[5]; all other values listed (droplet size, velocity, and temperature) are those for the calibrated region.[6] Ice growth at three different temperatures (+27, +10, and −10°F) is shown for both the heavy and light icing conditions. All results are for transducers located on the stagnation line of the test cylinder. The total ice accretion mechanically measured with outside calipers at the completion of each run is also plotted, if known. The accuracy of the ultrasonic pulse-echo thickness measurements was found to be within 0.5 mm (0.02 in.) of the "actual" accretion measured with the calipers for all runs where mechanical measurements were obtained. Since the pulse-echo measurement is made over the area of the transducer element, there will inevitably be some discrepancy between this measurement and a point thickness measurement, such as the caliper reading. The close agreement between the mechanically measured thicknesses and the ultrasonic measurements confirms previous experimental results[1-4] showing that the speed of propagation of the ultrasonic signal is insensitive to widely varying icing conditions. (The range of icing conditions for the tunnel tests comprised liquid water contents from 0.3 to 1.2 g/m^3 est., freestream airspeeds between 110 and 230 mph, median volume drop sizes from 12 to 20.5 μm, and cloud temperatures of +27, +10, and −10°F.)

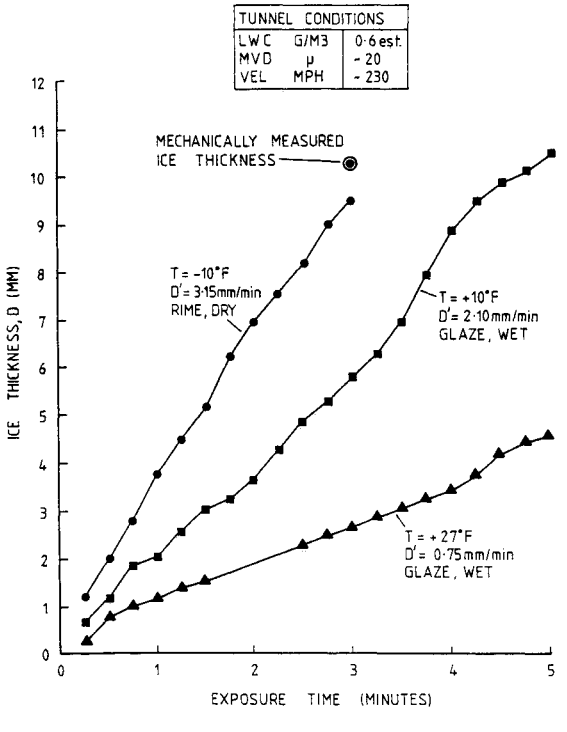

Fig. 7 Ice growth under "heavy" icing tunnel conditions.

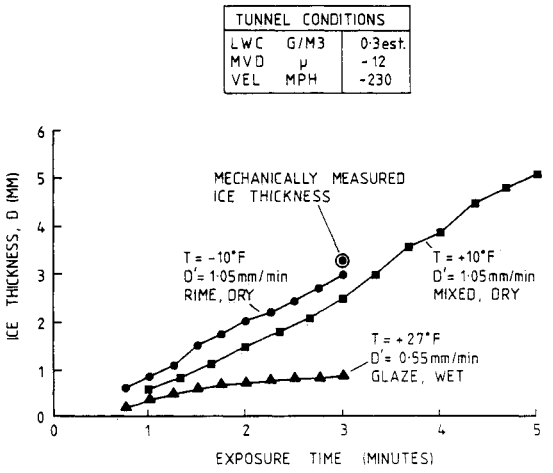

Fig. 8 Ice growth under "light" icing tunnel conditions.

The instantaneous ice accretion rate is simply the slope of the ice thickness curve at any point in time. The ice accretion rates measured in the IRT remain fairly constant throughout each run. This behavior is a result of the constant icing cloud conditions during each run and the transducer location on the cylinder stagnation line. Since ice accretion in the immediate vicinity of the cylinder stagnation line does not significantly change the flowfield in that region, and hence the local collection efficiency and heat-transfer coefficient, the ice accretion rate there can be expected to be approximately constant for a given set of icing cloud conditions.

While the accretion rates measured for constant icing cloud parameters are relatively uniform, the accretion rates measured under different icing cloud conditions differ significantly. As expected, the accretion rates measured under "heavy" icing conditions are greater than those observed under "light" icing conditions at the same temperature. For example, at −10°F the accretion rate is 3.15 mm/min (7.4 in./h) for the heavy icing conditions, while it is only 1.05 mm/min (2.5 in./h) for the light icing case. The higher accretion rates for each cloud temperature under heavy icing are simply caused by the higher impinging mass flux for these conditions. More interesting is the difference between accretion rates measured when only the temperature of the icing cloud was changed. At the relatively warm temperatures just below +32°F, the accretion rate is low. However, as the temperature of the icing cloud is progressively reduced, the accretion rate is observed to increase to a maximum value and then remain constant despite further decreases in icing cloud temperature. For example, for the light icing conditions, at +27°F the average accretion rate is 0.55 mm/min (1.3 in./h), at +10°F it is 1.05 mm/min (2.5 in./h), and at −10°F it is still 1.05 mm/min (2.5 in./h). This behavior represents the transition from wet to dry ice growth.

During wet ice growth the droplets impinging on the stagnation line do not completely freeze on impact, the heat of fusion released exceeding the rate at which heat is locally removed. Thus a fraction of the impinging mass flux runs back over the ice surface as liquid water. Heat is progressively removed from this runback liquid, primarily by convection, until it freezes at some point "downstream" of initial impact point. Liquid runback during wet growth therefore results in a lower accretion rate on the stagnation line than under dry

growth, when all of the droplets impinging on the stagnation line freeze there. This runback behavior is observed in both the light and heavy icing cases shown, with the accretion rate during wet growth consistently lower than the rate measured during dry growth at the same temperature. In all cases, the ultrasonic signal characteristics described earlier were used to determine whether the ice growth was wet or dry. As the temperature of the icing cloud decreases, and if all other cloud parameters (LWC, MVD, V) remain the same, then due to the increased heat transfer from the accreting surface, both by convection and evaporation, the freezing fraction will increase. When all of the impinging droplets freeze on impact with the accreting ice surface the freezing fraction is unity and the ice growth is "dry," i.e., there is no liquid present on the accreting ice surface.

Figure 9 is a plot of average accretion rate vs cloud temperature for the light and heavy icing results shown in Figs. 7 and 8. Each point is labeled according to the type of ice growth, wet or dry, occurring. For the light icing case, the accretion rate increases from 0.55 mm/min (1.3 in./h) during wet growth at +27°F to 1.05 mm/min (2.5 in./h) at +10°F during dry growth, and then remains constant as the icing cloud temperature is further decreased to −10°F. However, for the heavy icing conditions it can be seen that at +10°F the growth is still wet and the accretion rate increases from 2.10 mm/min (5.0 in./h) at +10°F to 3.15 mm/min (7.4 in./h) at −10°F. For these "heavy icing" conditions the heat transfer from the ice surface was still insufficient at +10°F to completely freeze the high impinging mass flux, and hence wet growth was observed. At −10°F the ice growth is dry and the accretion rate measured, 3.15 mm/min (7.4 in./h) is therefore the maximum value for those conditions.

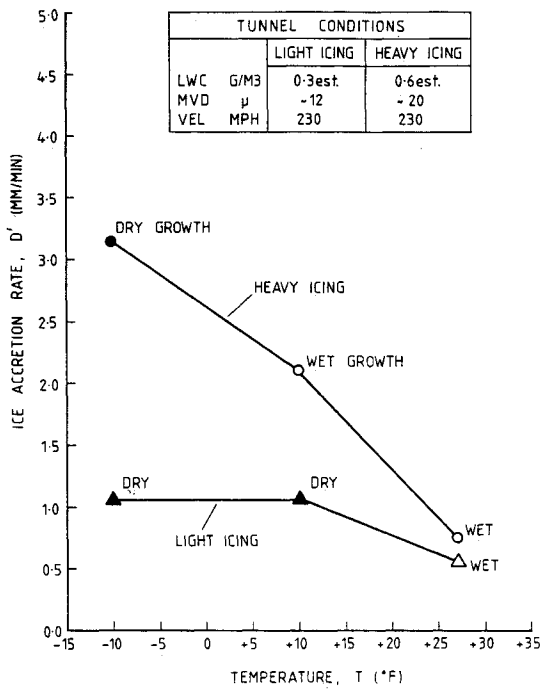

Fig. 9 Average ice accretion rate vs icing cloud temperature for "heavy" and "light" icing tunnel conditions.

Natural Icing Tests

Figure 10 contains a summary of the time-averaged icing conditions during each of the five in-flight exposures of the ultrasonic system (two exposures were made during flight 85-25). The shape of the accreted ice at the completion of each exposure was obtained from photographs of the iced cylinder. Also shown are the final ice thicknesses measured with the ultrasonic system and the outside calipers. The accuracy of the ultrasonic measurements is again seen to be within ±0.5 mm

TIME-AVERAGED ICING CONDITIONS

FLIGHT NUMBER	EXPOSURE TIME (MIN:SEC)	TEMP (°F)	LWC (GM/M3)	MVD (μ)	VEL (MPH)	ALTITUDE (FEET)
85-22	20:41	+22·3	0·36	11·9	157	2728
85-23	47:08	+26·1	0·18	11·4	147	3404
85-24	10:07	+5·7	0·46	14 est.	161	6480
85-25A	36:40	+4·8	0·19	14·1	167	7019
85-25B	11:29	+8·8	0·12	12·0	167	6837

FLIGHT NUMBER	ULTRASONICALLY MEASURED ICE THICKNESS (MM)	MECHANICALLY MEASURED ICE THICKNESS (MM)	ICE SHAPE
85-22	3·1	2·7	TRANSDUCER, FLOW, WET GROWTH
85-23	3·3	ICE SLID OFF	WET
85-24	8·9	8·7	DRY
85-25A	VIDEO TAPE DAMAGED	9·6	DRY
85-25B	1·0	1·3	DRY

Fig. 10 Summary of natural icing test results.

(±0.02 in.) of the mechanically measured ice thickness. For each exposure the type of ice growth, wet or dry, is also shown. The utrasonic signals during natural icing displayed the same characteristic echo patterns observed in the IRT tests, and were again used to determine the type of ice growth. The overall accretion rates encountered during the natural icing tests were much lower than those obtained at the relatively higher, constant liquid water contents used in the IRT tests. For example, only during flight 85-24 did the average accretion rate exceed 0.3 mm/min (0.7 in./h). For this reason, detailed ultrasonic measurements of ice thickness and ice accretion rate are only presented for flight 85-24.

Figure 11 shows ice thickness measured with the ultrasonic system plotted against exposure time for research flight 85-24. Ice thickness was calculated at 10 second intervals from the videotaped pulse-echo data; however, alternative data acquisition techniques would allow finer time resolution to be achieved, if desired. The time-averaged incing cloud conditions throughout the exposure are also listed. The ice growth for this exposure was dry, as indicated by the echo pattern received from the ice surface, an the average accretion rate was 0.88 mm/min (2.1 in./h).

Figure 12 is a plot of icing cloud and ice accretion data measured by existing instrumentation on the aircraft, as well as the ultrasonic system for flight 85-24. The upper plot shows "icing rate" (in millimeters per minute) measured by Rosemount and PIRAM ice detectors. Also shown is the ice accretion rate measured on the stagnation line of the test cylinder using the ultrasonic system. This accretion rate was determined by differentiating the measured ice accretion (Fig. 11) with respect to time. The lower plot shows the cloud liquid water content (in grams per cubic meter) measured by a Johnson-Williams hot-wire probe. Due to the cold cloud temperature and low liquid water content, dry ice growth was observed throughout the exposure. Under these conditions, and for a relatively constant droplet size distribution, icing rate is directly proportional to the cloud liquid water content. From Fig. 12

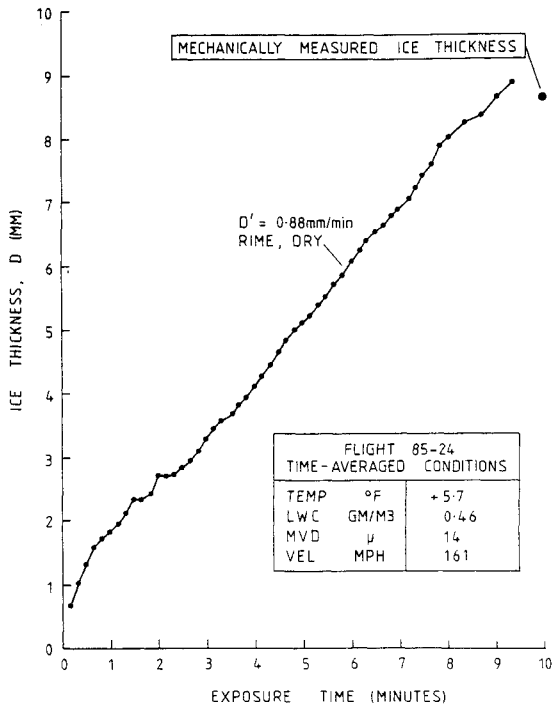

Fig. 11 Ice thickness vs exposure time for flight 85-24.

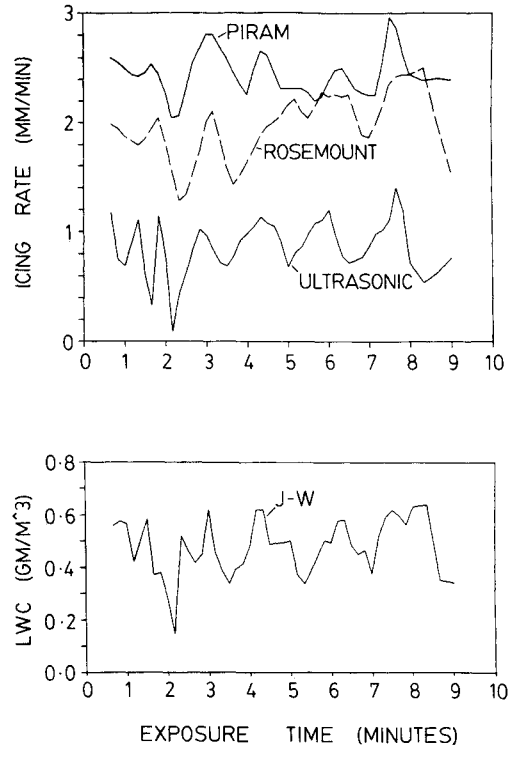

Fig. 12 Comparison of ice accretion rates measured by PIRAM, Rosemount, and ultrasonic ice detectors, and cloud liquid water content measured by a Johnson-Williams hot-wire probe for flight 85-24.

it can be seen that the three icing rate plots (Rosemount, PIRAM, and Ultrasonic) show an overall similarity to the LWC plot, e.g., all contain a decrease in icing rate after 2 min, corresponding to a decrease in the cloud liquid water content. However, the magnitudes of the icing rates indicated by the three instruments are markedly different, the PIRAM and Rosemount ice detectors indicating average icing rates of 2.45 and 1.96 mm/min, respectively, while the average ultrasonically measured accretion rate is 0.88 mm/min. The ultrasonically measured icing rate is consistent with the mechanically measured accretion of 8.7-mm on the test cylinder at the end of the 10-min exposure. The higher icing rates recorded by the PIRAM and Rosemount systems appear to be inconsistent with the cloud liquid water content measured by the Johnson-Williams probe. A regression line analysis of measured icing rate vs Johnson-Williams cloud liquid water content shows both PIRAM and Rosemount systems indicating, respectively, icing rates of 2.06 and 1.36 mm/min at zero liquid water content.

The PIRAM and Rosemount systems are both probe-type detectors that measure ice accumulation on a small, protruding probe.[7] The calibration of these systems depends upon the collection efficiency of the probe, which, in turn, varies with the cloud droplet size distribution. Since the ultrasonic system is noninvasive, ice thickness and icing rate are directly measured on the surface of interest and no calibration is required. Referring again to Fig. 12, it can be seen that the time variation of the liquid water content is recorded by the ultrasonic system, while the Rosemount and PIRAM plots do not contain the same level of detail, particularly beyond an exposure time of 4 min, with the Rosemount data showing an apparent drift to a higher icing rate. The time response of probe-type systems is generally limited by two factors: the amount of ice necessary to initiate the icing signal and the need to repeatedly thermally deice the probe. The response time of both the PIRAM and Rosemount instruments is, therefore, dependent on the severity of the icing conditions and also physically limited by the time taken to deice the probe (typically 5-7 s). The time response of the ultrasonic system is not limited by the need for deicing and does not depend on the icing severity; it is only fundamentally limited by the ultrasonic pulse repetition frequency, which is typically several kilohertz.

Figure 13 compares ice accretion measured in flight with ice accretion measured in the IRT under roughly similar icing cloud conditions. It should be remembered that the conditions listed for the IRT are only approximate, since the test cylinder was beyond the calibrated cloud region. However, the usefulness of such a comparison between ice growth under natural and simulated icing conditions in supporting icing research, both experimental and analytical, is readily apparent.

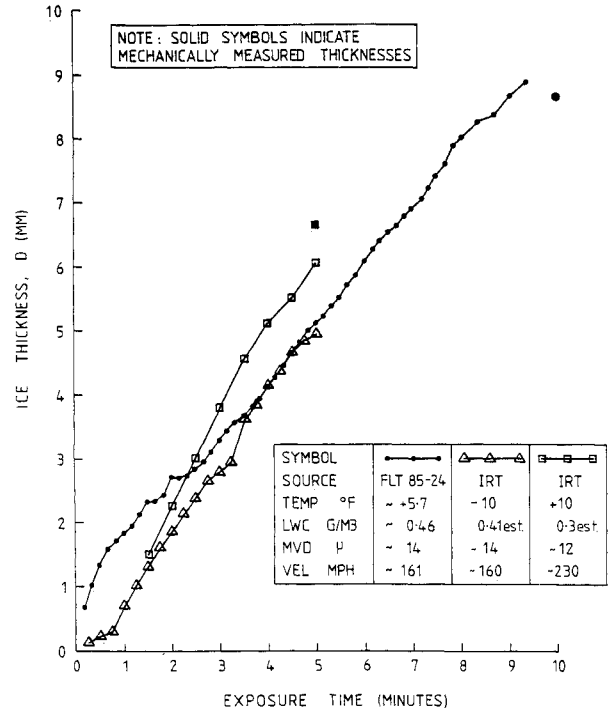

Fig. 13 Comparison of ice thickness vs exposure time for similar natural (flight 85-24) and tunnel (IRT) icing conditions.

Conclusions

Tests conducted on cylinders instrumented with ultrasonic transducers exposed to simulated and natural icing conditions have provided the following information:

1) Ultrasonic pulse-echo techniques can be used to provide a continuous measurement of ice thickness on an accreting body. Ice thickness was measured to within an accuracy of ± 0.5 mm (± 0.02 in.) using this technique.

2) The ultrasonic signals used for pulse-echo thickness measurement allow the following ice growth information to be determined:

a) Ice thickness, from the pulse-echo transit time through the ice.

b) Ice accretion rate, obtained by differentiating the measured thickness with respect to time.

c) The presence of liquid water on the surface of the ice, from the time variation of the surface echoes.

d) A measure of the surface roughness, from the width of the surface echoes received.

3) For dry ice growth in natural icing conditions, fluctuations in cloud liquid water content result in corresponding changes in ice accretion rate measured with the ultrasonic pulse-echo technique. The time response of existing probe-type detectors is both dependent on icing severity and limited by the need to repeatedly deice the probe. The time resolution achievable using ultrasonic pulse-echo techniques is potentially superior since ice thickness can be directly measured many times a second. The ultrasonic system requires no cloud-dependent calibration.

Ultrasonic pulse-echo techniques therefore offer the proven potential for the development of an operational instrument for detecting and monitoring aircraft icing as well as providing previously unobtainable data on the fine temporal and spatial characteristics of ice growth in simulated and natural icing conditions. In addition, the unique capability of the ultrasonic pulse-echo technique to detect the presence of liquid water on the accreting ice surface allows the threshold between wet and dry ice growth to be experimentally determined; from this "critical impingement" data valuable information about the heat transfer at the ice surface may be inferred.

Acknowledgments

This work was supported by the National Aeronautics and Space Administration and the Federal Aviation Administration under the Joint University Program for Air Transportation, Grant NGL-22-009-640. Wind-tunnel and flight-test facilities were provided by the NASA Lewis Research Center.

References

[1]Hansman, R.J. and Kirby, M.S., "Measurement of Ice Accretion Using Ultrasonic Pulse-Echo Techniques," *Journal of Aircraft,* Vol. 22, June 1985, pp. 530-535.

[2]Pounder, E.R., *Physics of Ice,* Pergamon Press, London, England, 1965.

[3]Kingery, W.D., *Ice and Snow,* MIT Press, Cambridge, MA, 1963, pp. 187-211.

[4]Yakovlev, G.N., *Studies in Ice Physics and Ice Engineering,* National Science Foundation Scientific Translations, Washington, D.C., 1971, p. 46.

[5]Personal communication with R.J. Shaw, NASA Lewis Research Center, Cleveland, OH, Jan. 1985.

[6]Personal communication with P.J. Perkins, NASA Lewis Research Center, Cleveland, OH, Jan. 1986.

[7]Ide, R.F. and Richter, G.P., "Comparison of Icing Cloud Instruments for 1982-1983 Icing Season Flight Program," NASA TM-83569, 1984.